Color chiral Cherenkov radiation and energy loss in the quark-gluon plasma

Jeremy Hansen and Kirill Tuchin●

Department of Physics and Astronomy, Iowa State University, Ames, Iowa 50011, USA

We introduce and investigate the color chiral Cherenkov effect which consists in radiation of the circularly polarized gluons by a fast color charge moving with constant velocity in the presence of the chiral magnetic current. We derive the transition rates for all gluon polarizations. We compute the contribution of the color chiral Cherenkov effect to the parton energy loss in the quark-gluon plasma.

I. INTRODUCTION

A fast particle carrying electric charge and moving in a medium with chiral fermions can lose a significant portion of its energy by means of the chiral Cherenkov radiation [1–4]. It is emitted due to the unique dispersion relation of the electromagnetic field and is closely related to the chiral magnetic [5–9] and anomalous Hall effects [8,10–13]. Thus far all studies of the chiral Cherenkov radiation focused on the media governed by the quantum electrodynamics because of possible technological applications. However, it is clear that the color version of the chiral Cherenkov effect is expected to give a significant contribution to the energy loss in strongly interacting media with chiral fermions. We therefore set in this paper to derive the color version of the chiral Cherenkov effect and estimate its magnitude in the quark-gluon plasma.

The color version of the chiral magnetic effect—the induction of the color current in the direction of the color magnetic field—can be described by letting the θ angle slowly vary with time. The gluon field excitations in the chiral medium supporting the chiral magnetic current are governed by the Lagrangian [14–16]

$$\mathcal{L} = -\frac{1}{2}\mathrm{Tr}(F_{\mu\nu}F^{\mu\nu}) - \frac{c_A}{2}\theta\,\mathrm{Tr}(F_{\mu\nu}\tilde{F}^{\mu\nu}), \qquad (1)$$

where the field tensor is

$$F_{\mu\nu} = \partial_\mu A_\nu - \partial_\nu A_\mu - ig[A_\mu, A_\nu]. \qquad (2)$$

$A_\mu = A_\mu^a t^a$ and $F_{\mu\nu} = F_{\mu\nu}^a t^a$, where t^a are the SU(3) generators. $\tilde{F}^{\mu\nu} = \frac{1}{2}\epsilon_{\mu\nu\lambda\rho}F^{\lambda\rho}$ is the dual field tensor. The

external pseudoscalar field θ is sourced by the topological charge and c_A is the anomaly coefficient.

The equations of motion derived from the Lagrangian (1) depend only on the gradient $\partial_\mu\theta$. We adopt a model of the quark-gluon plasma with spatially homogeneous and slowly time-dependent θ: $c_A\partial_\mu\theta = b_0\delta_{\mu 0}$, where b_0 is the (constant) chiral magnetic conductivity. As a result the chiral magnetic current $j^a = b_0 \boldsymbol{B}^a$ emerges as a source of the color magnetic field in Amper's law. That θ is a slow function of time is indicated by the parametrically large sphaleron transition time $1/(g^4 T)$ at a given plasma temperature T [17–19].

The chiral magnetic current modifies the spectrum of the gluon excitations, which can be found by solving the equations of motion without the self-interaction terms:

$$\partial_\nu F^{\mu\nu} + b_\nu \tilde{F}^{\mu\nu} = 0, \qquad (3)$$

along with the Bianchi identity. In the radiation gauge, the corresponding vector potential obeys the equation

$$\partial_t^2 \boldsymbol{A} - \nabla^2 \boldsymbol{A} = b_0(\boldsymbol{\nabla} \times \boldsymbol{A}). \qquad (4)$$

The plane wave solutions of (4) are circularly polarized and have the dispersion relation

$$\omega^2 = \boldsymbol{k}^2 - \lambda b_0 |\boldsymbol{k}|, \qquad (5)$$

where $k = (\omega, \boldsymbol{k})$ and $\lambda = \pm 1$ indicate the right or left polarization. With the account of the screening effects the in-medium gluons have the dispersion relation

$$\omega^2 = \boldsymbol{k}^2 + \mu^2(\boldsymbol{k}) = \boldsymbol{k}^2 - \lambda b_0|\boldsymbol{k}| + \omega_p^2, \qquad (6)$$

where μ is the gluon mass parameter and ω_p is the plasma frequency. Actually, Eq. (6) is the short wavelength limit of the full dispersion relation [20,21], which nevertheless suffices for the present calculation. Throughout the paper we assume that b_0 is positive. Since Eq. (6) scales with λb_0,
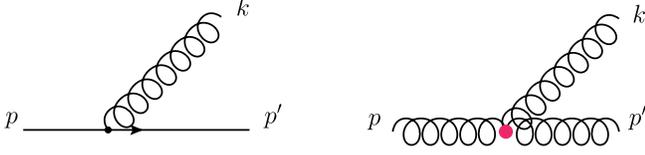
FIG. 1. $1 \rightarrow 2$ processes contributing to the color chiral Cherenkov radiation. The anomalous contributions come about by the way of the gluon dispersion relation (6) and as an extra term in the triple-gluon vertex (10). The latter fact is indicated by the big red circle.

the negative b_0 case can be obtained by the replacement $b_0 \rightarrow -b_0$ and $\lambda \rightarrow -\lambda$.

The chiral term in the gluon dispersion relation generates the spacelike gluon mode $\omega^2 - \mathbf{k}^2 < 0$ which opens the possibility for novel $1 \rightarrow 2$ processes that are otherwise prohibited in QCD by energy and momentum conservation. This effect is analogous to the Cherenkov radiation where the spacelike excitations of the electromagnetic field produced by a particle moving at a speed greater than the phase velocity of light represent the propagating wave solution in dielectric materials. In chiral media, the chiral conductivity effectively contributes to the medium dielectric response making possible excitation of the gauge field wave. This effect is referred to as the chiral Cherenkov radiation. We refer to its QCD version as the color chiral Cherenkov radiation.

Unlike QED, where the chiral Cherenkov radiation is described by a single diagram $e \rightarrow e\gamma$, where the photon dispersion relation is modified by the anomaly, in QCD there are two possible channels depicted in Fig. 1. The first of these channels $q \rightarrow qg$ is quasi-Abelian. The corresponding emission rate can be derived from the Abelian expression by including the appropriate color factors. We performed this calculation in [3]. The novel channel is $g \rightarrow gg$ where all three gluons are excitations of the chiral medium. It is the focus of the present article.

The paper is structured as follows. The next section deals with the Feynman rule for the triple-gluon vertex stemming from the second term in the right-hand side of (1). The main result, namely, the transition rates for all quark and gluon polarization states, is derived in Sec. III. Section IV discusses the energy loss due to the color chiral Cherenkov radiation. The summary and outlook are presented in Sec. V.

II. THE TRIPLE-GLUON VERTEX

The diagrams contributing to the color chiral Cherenkov radiation are depicted in Fig. 1. Whereas the anomaly does not affect the Feynman rule of the fermion-gluon vertex, it does modify the triple-gluon one. To derive the rule we write in the second term in (1)

$$\text{Tr}(F^{\mu\nu}\tilde{F}^{\mu\nu}) = 2\partial_\mu K^\mu, \tag{7}$$

where

$$K^\mu = \epsilon^{\mu\nu\rho\sigma}\text{Tr}\left(A_\nu \partial_\rho A_\sigma - g\frac{2i}{3}A_\nu A_\rho A_\sigma\right), \tag{8}$$

and integrate by parts the corresponding term in the action. The result is

$$S_\theta = c_A \int \partial_\mu \theta \epsilon^{\mu\nu\rho\sigma}\left(\frac{1}{2}A_\nu^a \partial_\rho A_\sigma^a - g\frac{2i}{3}\frac{1}{4}if^{abc}A_\nu^a A_\rho^b A_\sigma^c\right)d^4x. \tag{9}$$

The first term in (9) contributes to the equation of motion (3), while the second one to the triple-gluon vertex. The variation of action S_θ with respect to three gluon fields produces the Feynman rule for the anomalous contribution to the triple-gluon vertex in momentum space:

$$\text{anomalous triple-gluon vertex} = gb_\mu \epsilon^{\mu\nu\rho\sigma}f^{abc}, \tag{10}$$

where we follow the conventions of [22]. This is the only new Feynman rule due to the anomalous term in the Lagrangian (1). The red circle in Fig. 1 includes both the conventional and anomalous contributions.

III. THE CHIRAL CHERENKOV RADIATION RATE

The radiation rates can be computed as

$$dW_{a\rightarrow bc} = \frac{g^2 C_{a\rightarrow bc}}{2(2\pi)^2}\sum_{ss'}\delta(\omega + E' - E)\delta(\mathbf{k} + \mathbf{p}' - \mathbf{p})$$
$$\times \frac{1}{8EE'\omega}|\mathcal{M}_{a\rightarrow bc}|^2 d^3p'd^3k, \tag{11}$$

where the sum runs over the fermion polarization states, $\mathcal{M}_{a\rightarrow bc}$ are the amplitudes without color generators t^a and the structure constants f^{abc}, and $C_{a\rightarrow bc}$ are the color factors. The color factors are given by

$$C_{q\rightarrow qg} = \frac{1}{N_c}\text{tr}(t^a t^a) = \frac{N_c^2 - 1}{2N_c} = \frac{4}{3}, \tag{12}$$

$$C_{g\rightarrow gg} = \frac{(f^{abc})2}{N_c^2 - 1} = N_c = 3. \tag{13}$$

The matrix elements read

$$i\mathcal{M}_{q\rightarrow qg} = i\bar{u}_{\mathbf{p}'s'}\not{e}_{\mathbf{k}\lambda}^* u_{\mathbf{p}s}, \tag{14}$$

$$i\mathcal{M}_{g\rightarrow gg} = i\mathcal{M}_{g\rightarrow gg}^A + i\mathcal{M}_{g\rightarrow gg}^B$$
$$= (e_{\mathbf{p}\lambda_0} \cdot e_{\mathbf{k}\lambda}^*)(p + k) \cdot e_{\mathbf{p}'\lambda'}^* + (e_{\mathbf{k}\lambda}^* \cdot e_{\mathbf{p}'\lambda'}^*)(p' - k)$$
$$\cdot e_{\mathbf{p}\lambda_0} - (e_{\mathbf{p}\lambda_0} \cdot e_{\mathbf{p}'\lambda'}^*)(p + p') \cdot e_{\mathbf{k}\lambda}^*$$
$$- ib_\mu \epsilon^{\mu\nu\rho\sigma}e_{\mathbf{p}\lambda_0,\nu}e_{\mathbf{k}\lambda,\rho}^* e_{\mathbf{p}'\lambda',\sigma}^*, \tag{15}$$

where $e_{p\lambda\mu}$'s are the circular polarization vectors and the superscripts A and B refer to the second and third lines of (15), respectively. Note that not just the last line in (15), but all terms in (14) and (15) depend on the anomaly by the way of the dispersion relation (6).

We perform the calculation in the high-energy approximation, meaning that the momenta of all particles along the jet axis are much larger than the transverse momenta and the effective mass. Let z be the jet axis, and then

$$p = \left(E, 0, 0, E - \frac{k_\perp^2 + x(1-x)\mu^2(E)}{2x(1-x)E} \right), \quad (16a)$$

$$k = \left(\omega, k_\perp, 0, \omega - \frac{k_\perp^2 + \mu^2(\omega)}{2\omega} \right), \quad (16b)$$

$$p' = \left(E', -k_\perp, 0, E' - \frac{k_\perp^2 + \mu^2(E')}{2E'} \right), \quad (16c)$$

where the mass parameter in (6) becomes $\mu^2(\omega) \approx \omega_p^2 - \lambda b_0 \omega$ and $x = \omega/E$ is the fraction of energy of the incident parton carried away by the gluon k. Equations (16) assume that $k_\perp \ll E, E', \omega$ and $|\mu| \ll E, E', \omega$. The latter condition is equivalent to $b_0 \ll E, E', \omega$.

Given (16), the polarization vectors can be chosen as

$$e_{p\lambda_0} = \frac{1}{\sqrt{2}}(0, 1, \lambda_0 i, 0), \quad (17a)$$

$$e_{k\lambda} = \frac{1}{\sqrt{2}}\left(0, 1, \lambda i, -\frac{k_\perp}{\omega}\right), \quad (17b)$$

$$e_{p'\lambda'} = \frac{1}{\sqrt{2}}\left(0, 1, \lambda' i, \frac{k_\perp}{E'}\right). \quad (17c)$$

The integral over the p' in (11) is trivial considering the delta function expressing the momentum conservation. The remaining delta function in $q \to qg$ rate reads

$$\delta(E' + \omega - E) = 2x(1-x)E\delta\left[k_\perp^2 + \mu^2(\omega)(1-x) + m^2 x^2\right]$$
$$= 2x(1-x)E\delta\left[k_\perp^2 + (\omega_p^2 - \lambda b_0 xE)\right.$$
$$\left. \times (1-x) + m^2 x^2\right]. \quad (18)$$

Clearly, the argument of this delta function can vanish only if $\lambda b_0 > 0$. We assumed in the introduction that $b_0 > 0$. Therefore, only the right-polarized gluons $\lambda > 0$ can be radiated by the incident quark. Moreover, the energy conservation, expressed by the argument of the delta function (18), can be satisfied only if

$$x_-^{q\to qg} < x < x_+^{q\to qg}, \quad (19)$$

where

$$x_\pm^{q\to qg} = \frac{\omega_p^2 + \lambda b_0 E \pm \sqrt{(\omega_p^2 - \lambda b_0 E)^2 - 4m^2\omega_p^2}}{2(m^2 + \lambda b_0 E)}. \quad (20)$$

The requirement that (20) have real values sets the infrared threshold for the energy of the incident quark:

$$E > E_1 = \frac{2m\omega_p + \omega_p^2}{b_0}. \quad (21)$$

The delta function in $g \to gg$ rate reads

$$\delta(E' + \omega - E) = 2x(1-x)E\delta\left[k_\perp^2 + x\mu^2(E')\right.$$
$$+ (1-x)\mu^2(\omega) - x(1-x)\mu^2(E)\right]$$
$$= 2x(1-x)E\delta\left[k_\perp^2 + \omega_p^2(1-x+x^2)\right.$$
$$\left. - b_0 E(\lambda + \lambda' - \lambda_0)x(1-x)\right]. \quad (22)$$

In this case the gluon emission is possible only if $\lambda + \lambda' > \lambda_0$. Apparently only the following four channels are allowed: $g_L \to g_R g_L$, $g_L \to g_L g_R$, $g_R \to g_R g_R$, and $g_L \to g_R g_R$. In the first three of these channels $\lambda + \lambda' - \lambda_0 = 1$, whereas in the last one $\lambda + \lambda' - \lambda_0 = 3$. Additionally,

$$x_-^{g\to gg} < x < x_+^{g\to gg}, \quad (23)$$

where

$$x_\pm^{g\to gg} = \frac{\omega_p^2 + (\lambda + \lambda' - \lambda_0)b_0 E \pm \sqrt{(\omega_p^2 - (\lambda + \lambda' - \lambda_0)b_0 E)^2 - 4\omega_p^4}}{2(\omega_p^2 + (\lambda + \lambda' - \lambda_0)b_0 E)}. \quad (24)$$

The requirement that (24) have real values sets the infrared threshold for the energy of the incident gluon:

$$E > E_2 = \frac{3\omega_p^2}{b_0}. \quad (25)$$

The amplitude $\mathcal{M}_{q \to qg}$ was computed in [1]:

$$\sum_{ss'} |\mathcal{M}_{q \to qg_R}|^2 = 4\left[EE' - m^2 - \frac{(\boldsymbol{k} \cdot \boldsymbol{p})(\boldsymbol{k} \cdot \boldsymbol{p'})}{k^2}\right], \quad (26)$$

$$\sum_{ss'} |\mathcal{M}_{q \to qg_L}|^2 = 0. \quad (27)$$

For the gluon splitting amplitudes we find

$$i\mathcal{M}^A_{g_R \to g_R g_R} = \frac{k_\perp}{x(1-x)}, \quad (28a)$$

$$iM^A_{g_L \to g_R g_L} = \frac{(1-x)k_\perp}{x}, \quad (28b)$$

$$iM^A_{g_L \to g_L g_R} = \frac{x k_\perp}{(1-x)}, \quad (28c)$$

$$iM^A_{g_L \to g_R g_R} = \mathcal{O}(k_\perp^2/E, b_0/E), \quad (28d)$$

$$iM^B_{g \to gg} = \frac{-b_0 k_\perp(\lambda(1-x) + \lambda' x + \lambda_0)}{x(1-x)E}, \quad (28e)$$

provided that $k_\perp, b_0 \ll E, E', \omega$. In the high-energy limit $\mathcal{M}^B_{gg}$ appears only as a subleading correction to $\mathcal{M}^A_{g \to gg}$ and therefore can be neglected in our calculation. We note, incidentally, that $\mathcal{M}^B_{g_L \to g_R g_R} = 0$ so that the anomalous vertex correction does not contribute even in the subleading channel (28d). Substituting (26), (28), (12), and (13) into (11) and summing over the final gluon polarizations we derive

$$\frac{dW_{q \to qg}}{dk_\perp^2 dx} = \frac{\alpha_s g^2}{3x^2(1-x)E}\left[(1 + (1-x)^2)k_\perp^2 + m^2 x^4\right]$$
$$\times \delta(k_\perp^2 + \mu^2(1-x) + m^2 x^2), \quad (29a)$$

$$\frac{dW_{g_R \to gg}}{dk_\perp^2 dx} = \frac{3\alpha_s g^2}{2x^2(1-x)^2 E} k_\perp^2 \delta(k_\perp^2 + \omega_p^2 x^2$$
$$+ (\omega_p^2 - b_0 \omega)(1-x)), \quad (29b)$$

$$\frac{dW_{g_L \to gg}}{dk_\perp^2 dx} = \frac{3\alpha_s g^2}{2E}\left[\frac{(1-x)^2}{x^2} + \frac{x^2}{(1-x)^2}\right] k_\perp^2 \delta(k_\perp^2 + \omega_p^2 x^2$$
$$+ (\omega_p^2 - b_0 \omega)(1-x)). \quad (29c)$$

One can easily identify in (29) the contributions to the standard splitting functions $P_{gq}(x)$ and $P_{gg}(x)$ corresponding to gluon emission. Integrating over the transverse momentum $k_\perp$ we obtain the spectra of the gluon emission rate:

$$\frac{dW_{q \to qg}}{dx} = \frac{\alpha_s g^2}{3x^2 E}\left\{[1 + (1-x)^2](b_0 xE - \omega_p^2) - 2m^2 x^2\right\}$$
$$\times \Theta(x_+^{q \to qg} - x)\Theta(x - x_-^{q \to qg}), \quad (30a)$$

$$\frac{dW_{g_{\lambda_0} \to gg}}{dx} = \frac{3\alpha_s g^2}{4x^2(1-x)^2 E}\left\{(b_0 E - \omega_p^2)(1-x) - \omega_p^2 x^2\right\}$$
$$\times \left\{[x^4 + (1-x)^4]\delta_{\lambda_0, -1} + \delta_{\lambda_0, 1}\right\}$$
$$\times \Theta(x_+^{g \to gg} - x)\Theta(x - x_-^{g \to gg}). \quad (30b)$$

Here Θ is the Heaviside step function, and $\lambda_0 = \pm 1$ is the right- and left-hand polarizations of the incident gluon.

IV. COLOR CHIRAL CHERENKOV RADIATION IN QUARK-GLUON PLASMA

We now consider the rate of gluon radiation due to the color chiral magnetic current in quark-gluon plasma. The plasma frequency and the quark thermal mass are given by $\omega_p^2 = \frac{g^2 T^2}{18}(2N_c + N_f)$ and $m^2 = \frac{g^2 T^2}{16 N_c}(N_c^2 - 1)$, respectively [23]. Using these equations in (30) we compute the anomalous contribution to the gluon emission spectra from quark-gluon plasma shown in Fig. 2. We emphasize that
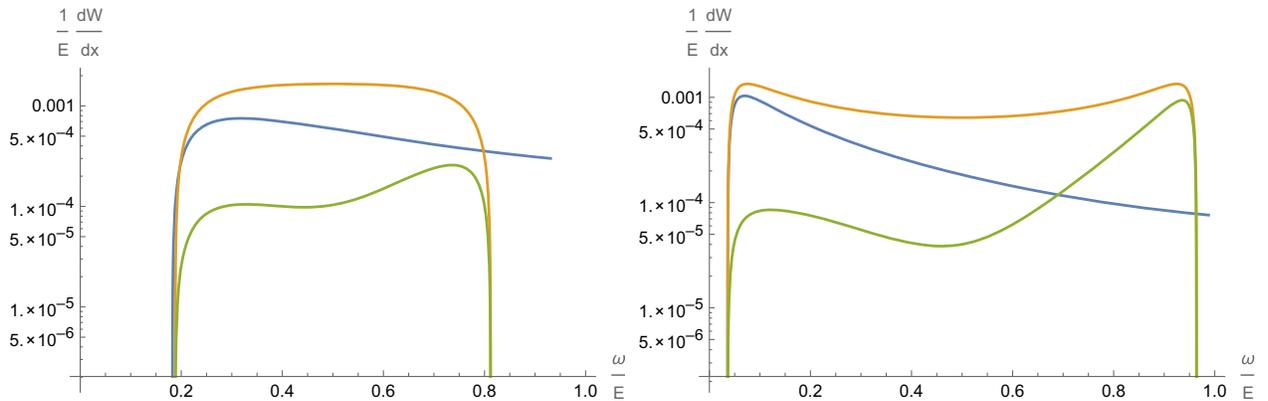
FIG. 2. The color chiral Cherenkov radiation rates versus $x = \omega/E$. The channels $q \to qg$, $g_R \to gg$, and $g_L \to gg$ are represented by blue, orange, and green lines, respectively. Left panel: $E = 20$ GeV; right panel: $E = 100$ GeV. Both panels: $g = 2$, $T = 300$ MeV, and $b_0 = 50$ MeV.

this calculation takes into account only the anomaly-induced radiation which is but a fraction of the total gluon radiation. One can observe that the gluon spectrum is constrained by the thresholds (20) and (24). The thresholds nearly coincide in the infrared but are different in the ultraviolet part of the spectrum. The right-handed gluons decay most readily except in the far infrared which is dominated by the radiation off the quark.

The contribution of the color chiral Cherenkov radiation to the energy loss by a fast parton propagating in quark-gluon plasma along the z axis is given by

$$-\frac{dE_{a\to bc}}{dz} = \int_0^E \omega \frac{dW_{a\to bc}}{d\omega} d\omega$$

$$= E \int_0^1 x \frac{dW_{a\to bc}}{dx} dx. \qquad (31)$$

Substituting (30) into (31) yields for each channel

$$-\frac{dE_{q\to qg}}{dz} = \frac{2\alpha_s g^2}{3} \left\{ \left(x_+^{q\to qg} - x_-^{q\to qg}\right) \left[\left(x_+^{q\to qg} + x_-^{q\to qg} - 8\right)\right.\right.$$
$$\left.\times b_0 E - 8m^2 - 2\omega_p^2\right]$$
$$\left. + (b_0 E + \omega_p^2) \ln\frac{x_+^{q\to qg}}{x_-^{q\to qg}} \right\} \Theta(E - E_1), \qquad (32a)$$

$$-\frac{dE_{g_R\to gg}}{dz} = \frac{3\alpha_s g^2}{4} \left\{ (b_0 E - \omega_p^2) \ln\frac{x_+^{g\to gg}}{x_-^{g\to gg}} - 2(b_0 E + \omega_p^2)\right.$$
$$\left.\times \left(x_+^{g\to gg} - x_-^{g\to gg}\right) \right\} \Theta(E - E_2), \qquad (32b)$$

$$-\frac{dE_{g_L\to gg}}{dz} = \frac{\alpha_s g^2}{4} \left\{ \frac{3[(b_0 E + 2\omega_p^2)^2 - \omega_p^4]}{b_0 E + \omega_p^2} \ln\frac{x_+^{g\to gg}}{x_-^{g\to gg}}\right.$$
$$\left. - \left(17 b_0 E + 21\omega_p^2\right)\left(x_+^{g\to gg} - x_-^{g\to gg}\right) \right\}$$
$$\times \Theta(E - E_2). \qquad (32c)$$

In the high-energy limit $b_0 E \gg m^2, \omega_p^2$ Eqs. (32) simplify as follows:

$$-\frac{dE_{q\to qg}}{dz} = \frac{4\alpha_s g^2 b_0 E}{9}, \qquad (33a)$$

$$-\frac{dE_{g_R\to gg}}{dz} = \frac{3\alpha_s g^2 b_0 E}{4} \left(\ln\frac{b_0 E}{\omega_p^2} - 1\right), \qquad (33b)$$

$$-\frac{dE_{g_L\to gg}}{dz} = \frac{3\alpha_s g^2 b_0 E}{4} \left(\ln\frac{b_0 E}{\omega_p^2} - \frac{17}{6}\right). \qquad (33c)$$

Figure 3 exhibits the contribution of the color chiral Cherenkov radiation to the parton energy loss. We observe in that at high energy the right-hand gluon loses more energy than the left-handed one and the quark, while at
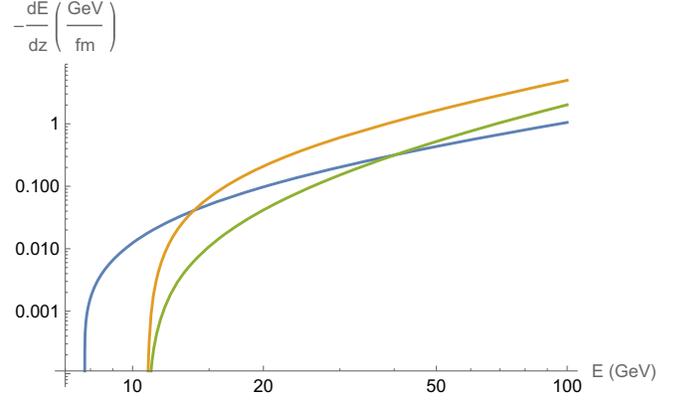
FIG. 3. The rate of energy loss due to the color chiral Cherenkov radiation for $q \to qg$ (blue), $g_R \to gg$ (orange), and $g_L \to gg$ (green). Parameters: $g = 2$, $T = 300$ MeV, and $b_0 = 50$ MeV.

lower energy the quark channel is the main mechanism of energy loss.

The energy loss of a jet consisting of many $q, \bar{q}, g$ states is determined by solving the system of coupled evolution equations for the parton distribution functions. Suppose that $f_a(x)$ are the momentum distribution functions of a species $a = q, \bar{q}, g$ normalized as

$$\sum_a \int_0^1 f_a(x) x dx = 1. \qquad (34)$$

Then, the jet energy loss is

$$-\frac{dE}{dz} = \sum_a \int_0^1 dx f_a(x) \left(-\frac{dE_a}{dz}\right), \qquad (35)$$

where the partial energy losses are given by Eqs. (32). Of course, jet energy loss due to the chiral anomaly is only a fraction of the total energy loss and therefore its phenomenological significance can be assessed only by incorporating the anomaly-induced corrections into the standard evolution equations.

V. SUMMARY AND OUTLOOK

We investigated the color chiral Cherenkov radiation—the QCD analog of the chiral Cherenkov effect in QED—and applied the results to study its role in the energy loss and jet quenching in the quark-gluon plasma. Our main result is the gluon emission rates (30) by quark and gluons in the chiral medium. The resulting energy loss is given by Eqs. (32).

A number of approximations were made to derive these results. Firstly, we assumed that the medium is homogeneous such that $\boldsymbol{b} = c_A \boldsymbol{\nabla}\theta = 0$. One can consider a complementary scenario where $\boldsymbol{b}$ is finite and b_0 vanishes. The corresponding rate of gluon emission by a fast quark

can be obtained similarly to QED, by substituting $b_0 \to |\boldsymbol{b}| \cos\beta$ where β into (30) is the angle between $\boldsymbol{b}$ and the outgoing gluon [1,4]. Gluon radiation by a fast gluon at finite $\boldsymbol{b}$, on the other hand, requires further analysis. However, it should be noted that while $\mathcal{M}^B_{g\to gg}$ gives a subrelativistic correction in a homogeneous medium, it gives no contribution at all in the inhomogeneous case. Indeed, the scattering amplitude $\mathcal{M}^B_{g\to gg} = -ib_\mu \epsilon^{\mu\nu\rho\sigma} e_{\boldsymbol{p}\lambda_0,\nu} e^*_{\boldsymbol{k}\lambda,\rho} e^*_{\boldsymbol{p}'\lambda',\sigma}$ is antisymmetric with respect to exchange of b_μ and any polarization vector. As such if $b_0 = 0$, then $\mathcal{M}^B_{g\to gg}$ must be proportional to the zeroth component of one of the polarization vectors. Therefore, given that the zeroth component is zero [see Eq. (17)], $\mathcal{M}^B_{g\to gg}$ vanishes.

Secondly, we assumed that the radiating particle is ultrarelativistic throughout the entire process. As a result, the spectrum in the quark channel exhibits discontinuous behavior at $x = x^{q\to qg}_+$, as can be seen in Fig. 2. By including nonrelativistic corrections for the outgoing particle, one may expect the rate of gluon emission to drop smoothly to zero as x tends to 1. This correction has very little effect on the rate of energy loss; however, it may play a role in parton evolution of jet.

Comparing the decay rates of the left-handed and right-handed gluons in Fig. 2, one finds that in a medium with $b_0 > 0$ the left-handed gluons decay more slowly when compared to right-handed ones. As a result jets develop strong left-hand polarization. This is the clearest manifestation of the chiral anomaly in the jet structure.

The chiral imbalance is also imprinted into the jet loss pattern seen in Fig. 3: the right-handed gluons lose a lot more energy than the left-handed ones. However, as the jet energy increases, the difference between the gluon polarizations becomes less pronounced since the energy loss is driven primarily by the large polarization-independent logarithms in (33). These logarithms also enhance the relative contribution of gluons as compared to quarks to the energy loss at high energies. In contrast, at low energy, the energy loss is dominated by quarks as seen in Fig. 3. We stress again that these conclusions hold only for energy loss due to the color chiral Cherenkov radiation and ignored all other contributions. A recent review of the conventional mechanisms of energy loss can be found in [24].

In conclusion, energy loss due to the color chiral Cherenkov radiation is significant. Therefore a comprehensive phenomenological analysis requires incorporation of the novel energy loss channels into the numerical packages describing jets in hot nuclear medium.

ACKNOWLEDGMENTS

[1] K. Tuchin, Phys. Lett. B **786**, 249 (2018).

[2] X.-G. Huang and K. Tuchin, Phys. Rev. Lett. **121**, 182301 (2018).

[3] J. Hansen and K. Tuchin, Phys. Rev. C **104**, 034903 (2021).

[4] K. Tuchin, Phys. Rev. D **98**, 114026 (2018).

[5] D. Kharzeev, Phys. Lett. B **633**, 260 (2006).

[6] D. E. Kharzeev, L. D. McLerran, and H. J. Warringa, Nucl. Phys. **A803**, 227 (2008).

[7] D. E. Kharzeev, Ann. Phys. (Amsterdam) **325**, 205 (2010).

[8] D. Kharzeev and A. Zhitnitsky, Nucl. Phys. **A797**, 67 (2007).

[9] K. Fukushima, D. E. Kharzeev, and H. J. Warringa, Phys. Rev. D **78**, 074033 (2008).

[10] F. R. Klinkhamer and G. E. Volovik, Int. J. Mod. Phys. A **20**, 2795 (2005).

[11] A. A. Zyuzin and A. A. Burkov, Phys. Rev. B **86**, 115133 (2012).

[12] A. G. Grushin, Phys. Rev. D **86**, 045001 (2012).

[13] D. E. Kharzeev, Prog. Part. Nucl. Phys. **75**, 133 (2014).

[14] F. Wilczek, Phys. Rev. Lett. **58**, 1799 (1987).

[15] S. M. Carroll, G. B. Field, and R. Jackiw, Phys. Rev. D **41**, 1231 (1990).

[16] P. Sikivie, Phys. Lett. B **137**, 353 (1984).

[17] P. B. Arnold, D. Son, and L. G. Yaffe, Phys. Rev. D **55**, 6264 (1997).

[18] P. B. Arnold, D. T. Son, and L. G. Yaffe, Phys. Rev. D **59**, 105020 (1999).

[19] D. Bodeker, Phys. Lett. B **426**, 351 (1998).

[20] Y. Akamatsu and N. Yamamoto, Phys. Rev. Lett. **111**, 052002 (2013).

[21] C. Manuel and J. M. Torres-Rincon, Phys. Rev. D **89**, 096002 (2014).

[22] M. E. Peskin and D. V. Schroeder, *An Introduction to Quantum Field Theory* (Addison-Wesley, Reading, MA, 1995).

[23] D. H. Rischke, Prog. Part. Nucl. Phys. **52**, 197 (2004).

[24] S. Cao and X.-N. Wang, Rep. Prog. Phys. **84**, 024301 (2021).